Acta Derm Venereol 2011; 91: 398–403

INVESTIGATIVE REPORT

Fluorescence Diagnostics of Basal Cell Carcinomas Comparing Methyl-aminolaevulinate and Aminolaevulinic Acid and Correlation with Visual Clinical Tumour Size

Carin SANDBERG[1], John PAOLI[1], Martin GILLSTEDT[1], Christina B. HALLDIN[1], Olle LARKÖ[1], Ann-Marie WENNBERG[1] and Marica B. ERICSON[1,2]

[1]*Department of Dermatology, Sahlgrenska Academy, and* [2]*Department of Physics, University of Gothenburg, Gothenburg, Sweden*

Fluorescence diagnostics based on aminolaevulinic acid (ALA) fluorescence has been suggested as an *in vivo* pre-surgical tool for tumour demarcation. We performed fluorescence diagnostics of 35 basal cell carcinomas (BCCs) undergoing photodynamic therapy (PDT) using methyl-aminolaevulinate (MAL). In addition, a semi-automated thresholding algorithm was implemented to detect the potential tumour region. The mean tumour fluorescence contrast was found to be 1.65 ± 0.06 during the first MAL-PDT session, and increased to 1.84 ± 0.07 at the second treatment ($p < 0.01$). This could imply that disruption of the skin barrier and inflammatory responses after the first session of PDT led to higher accumulation of protoporphyrin IX during the second session of PDT. The tumour areas detected based on fluorescence in small BCCs (< 1 cm^2) were in general ($n = 18/23$) larger than the visual clinical tumour size. In addition, the fluorescence contrast using MAL (1.65 ± 0.06) was found to be significantly higher ($p < 10^{-4}$) than the contrast (data from previous study) after application of ALA (1.20 ± 0.06). Thus, MAL generally provides higher tumour contrast than ALA in BCCs, and should be preferred for use in fluorescence diagnostics. Correlation between fluorescence, lack of treatment response and/or pain was not observed. ***Key words: aminolaevulinic acid; fluorescence diagnostics; fluorescence contrast; methyl-aminolevulinate; PDT; photodynamic therapy.***

(Accepted November 18, 2010.)

Acta Derm Venereol 2011; 91: 398–403.

Carin Sandberg, Department of Dermatology, Sahlgrenska Academy, University of Gothenburg, SE-413 45 Gothenburg, Sweden. E-mail: carin.sandberg@vgregion.se

The incidence rate of non-melanoma skin cancer has increased globally during the last few decades (1–3) and basal cell carcinoma (BCC) accounts for approximately 80% of these tumours (4–6). Photodynamic therapy (PDT) has become a popular therapeutic method for treatment of both superficial and thin nodular BCCs, with excellent cosmetic outcome (7, 8). After topical application of aminolaevulinic acid (ALA) or methyl aminolaevulinate (MAL), protoporphyrin IX (PpIX) is accumulated in the tumour through synthesis of cellular heme (9). Subsequent irradiation with red light induces a phototoxic reaction that kills the tumour cells. PDT has been shown to have equivalent cure rates compared with cryosurgery for superficial BCCs, but superior healing and cosmesis (10).

The general practice in Europe is to treat superficial BCCs with MAL-PDT twice, with an interval of one week between treatments (7, 8); however, it has not been investigated whether the degree of photosensitization differs between the two consecutive treatments. In acne, patients have been found to have a significantly lower PpIX fluorescence at the second treatment (11), but to our knowledge, no such study has been performed on BCCs. Furthermore, regardless of the type of PDT procedure, some BCCs will not respond to treatment (7). It is possible that the poor response of some BCCs can be explained by lack of PpIX accumulation, but this has not been studied.

In connection to PDT, a diagnostic technique based on fluorescence has evolved, so-called fluorescence diagnostics (FD) (12). By recording the red PpIX fluorescence of ALA-treated BCCs during illumination of blue light (wavelength (λ) = 365–405 nm) the tumour can be visualized (13–15). This technique can be used as an *in vivo* pre-surgical diagnostic tool, which can help to detect occult tumour borders of ill-defined BCCs before Mohs micrographic surgery (13). In order to obtain a good demarcation with FD, it is important that the fluorescence contrast between the tumour and the surrounding normal skin is as high as possible. There have been indications that PpIX formation is more tumour-selective when using MAL compared with ALA (16, 17), but clinical data verifying this are scarce. Data from a previous study by our group (14) were available in which the fluorescence contrast after ALA application to BCCs had been investigated. Since similar fluorescence data for MAL were lacking, the present study was designed to be able to compare the results with the earlier ALA data.

In this study, the objective was to evaluate the fluorescence contrast in superficial BCCs. Fluorescence images were obtained in connection with both the first and second

PDT sessions. The obtained MAL fluorescence contrast between the tumour and normal skin was also compared with data from our former study, in which ALA was used as the pro-drug. Furthermore, a refined semi-automated image analysis technique was implemented to identify the areas in the fluorescence images corresponding to tumour and to surrounding normal skin.

MATERIALS AND METHODS

Patients

Twenty-four patients (mean age 67 years, age range 36–86 years, 13 men and 11 women) with one or more clinically suspected superficial BCCs who were referred to the routine PDT-clinic were included in this clinical study. Two patients discontinued the study prematurely after the first PDT session, due to pain in one case and for unclear reasons in the other. Thus, 22 patients with 35 lesions in total were included for further analysis. The mean number of lesions per patient was 1.6 (range 1–6). Seventeen of the 35 lesions were histopathologically verified as superficial BCCs. All patients were referred for MAL-PDT at the clinic. The study was performed at the Department of Dermatology at Sahlgrenska University Hospital, Gothenburg, Sweden, and approved by the human ethics committee at the University of Gothenburg. All patients provided informed consent before any study-related procedures were undertaken. In an earlier study by our group (14), a comparable investigation of the fluorescence of BCCs treated with ALA was carried out on 40 patients with 40 lesions using the same fluorescence imaging device, as described below.

PDT procedure

All lesions were documented and photographed at all visits. The lesions were pre-treated with a light curettage to remove scales and crusts, taking care to avoid bleeding. The MAL cream (160 mg/g, Metvix®, Photocure, Oslo, Norway) was administered to the tumour in an approximately 1 mm thick layer, including at least a 1 cm surrounding margin. The area with the MAL cream was then occluded with a thin plastic film (Tegaderm®, 3M, UK). After 3 h, the film was removed and all superfluous cream wiped off gently. FD was performed (as described below) before the lesions were irradiated with red light using a light-emitting diode (LED)-lamp (Actilite®, Photocure, Oslo, Norway) with a wavelength centred around 635 nm, a fluence rate of 37 mW/cm^2 and a total light dose of 37 J/cm^2 according to the manufacturer's specifications. The patients were treated with two sessions on mean 8.3 days apart from each other (range 7–15).

Assessment of pain

The patients were asked to state their maximum pain experienced during both treatments by using a visual analogue scale (VAS), ranging from 0 (no pain) to 10 (unbearable pain).

Fluorescence diagnostics

All patients were subject to FD after application of MAL, but before the irradiation with red light at both treatment occasions. A photodemarcation system 1, prototype 5, (Medeikonos AB, Gothenburg, Sweden) was used for imaging the PpIX fluorescence. The system uses an excitation light generated by filtered mercury lamps, resulting in ultraviolet (UV)-blue light mainly concentrated in two peaks, at around 365 and 405 nm, having a fluence rate of 0.5 mW/cm^2. The detector consists of a filtered charged-coupled device (CCD)-camera, which records the fluorescence emission in the range of 610–715 nm, matching the PpIX emission at 635 nm. The fluorescence data consists of 8-bit grey-scale images (512 × 446 pixels), where the value of each pixel represents the measured fluorescence intensity at that point.

Follow-up

The patients were followed up 7–18 weeks after the second treatment. The treatment outcome was assessed as completely cleared, partially cleared (approximately 50%) or not cleared. Any adverse events were recorded.

Image analysis

All images and clinical photographs were analysed using Adobe® Photoshop® CS2 (Adobe Systems Incorporated, San José, California, USA) and Matlab® 7 Image processing toolbox (Mathworks Inc., Natick, MA, USA). The fluorescence images were converted to 16-bit format. The visual clinical margins of the BCCs were marked by a clinician on the digital photographs using Adobe® Photoshop® CS2. To detect the tumour margins in the fluorescence images a semi-automated thresholding algorithm was implemented in Matlab®, as described below.

A region of interest (ROI) was selected in each of the fluorescence images. The ROI was chosen as a region with even illumination, comprising the MAL-treated area including the lesion. A thresholding algorithm was implemented so that three regions in each image were identified; the highly fluorescent area presumably corresponding to the tumour area is delimited by the threshold denoted t_{tumour}; a surrounding medium fluorescent area corresponding to the MAL-treated area with normal skin delimited by thresholds t_{tumour} and t_{normal}; and outside t_{normal} a region with low fluorescence presumably without traces of the photosensitizer corresponding to the baseline fluorescence. The semi-automatic thresholding algorithm was based on the following. The total area of the regions within an image with an intensity that is higher than a certain threshold (t) is denoted by $A(t)$. By increasing the threshold (t), the area $A(t)$ will decrease. By investigating how $A(t)$ varies as a function of t in each image, the following quantity: $R(t)=1/A(t)\ \mathrm{d}A(t)/\mathrm{d}t$ can be determined, corresponding to the relative area change. Thus, the thresholds were selected so that the relative area change $R(t)$ assumed local maxima. The region was chosen by automatically detecting the local maxima of $R(t)$ and visually inspecting the fluorescence images, so that unrealistic thresholds were avoided. An example of how the thresholding algorithm operates is presented in Fig. 1. Fig. 1a illustrates a topographic view of a fluorescence image. The different thresholds were set to an intensity level at which the relative area change had a maximum, as illustrated by Fig. 1c. At this level, the slope of the topographic image was the steepest; see the location of the threshold planes in Fig. 1a. The corresponding thresholds marked in the fluorescence image are visualized in Fig. 1b. These areas were compared to investigate how the visual clinical area of the BCC corresponded to the area obtained from the fluorescence imaging.

After extracting the areas corresponding to the tumour area (T), normal MAL-treated skin (N) and baseline (B) using the semi-automatic segmentation program, the mean intensity (I) in the selected regions was calculated. Thereafter, the fluorescence contrast, defined as: $\kappa=I_T/I_N$ could be calculated. The area of the detected tumour region was also compared with the visual clinical tumour markings, and their correlation was assessed.

Statistics

Student's t-test and Wilcoxon's signed rank test were used as statistical methods. Pearson's correlation coefficient and

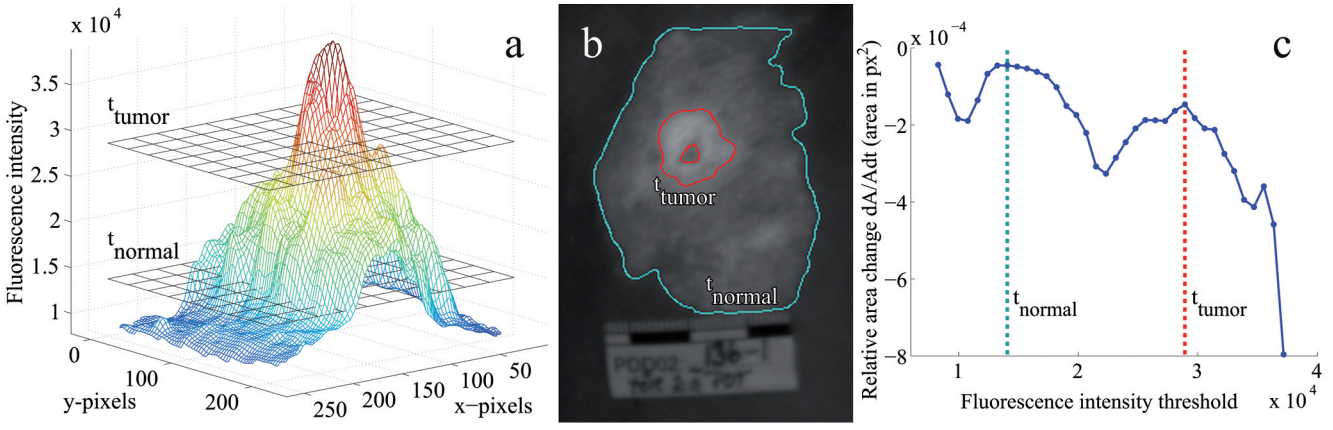

Fig. 1. Illustration of the semi-automated thresholding algorithm applied to fluorescence data of a basal cell carcinoma after topical application of methyl-aminolaevulinate. (a) The topographic view of the fluorescence data, where the fluorescence intensity is plotted as a three-dimensional surface. The z-coordinates equal the fluorescence intensities of the pixels located at the corresponding x,y coordinates in the image. The automated thresholds derived by the algorithm, t_{tumour} and t_{normal}, are marked with two planes intersecting the surface. (b) The fluorescence image to which the automated thresholds have been applied. The red margin corresponds to the threshold set by t_{tumour}, and the blue margin corresponds to t_{normal}. (c) The relative area change as a function of threshold. The two thresholds, t_{tumour} and t_{normal}, are chosen where the function has local maxima.

Spearman's rho were used to test for correlations. Three fluorescence images were excluded from the analysis since the selected ROI were found to contain areas with field cancerization and actinic keratoses. Fluorescence contrast data is presented as mean values ± standard error of the mean (SEM).

RESULTS

Fig. 1 shows the principles of the semi-automated thresholding algorithm used in this study (see also Material and Methods). Fig. S1 (available at: http://www.medicaljournals.se/acta/content/?doi=10.2340/00015555-1068) illustrates clinical photographs and fluorescence images of three different superficial BCCs obtained in connection with the two consecutive MAL-PDT sessions. The visual margins of the tumours are marked on the clinical photographs (first row). The typical crust formation obtained after PDT is observed in the lesions before the second treatment (row 3). The lesions were completely cleared at follow-up (row 5). Included in the fluorescence images (row 2 and 4) are also the borders between the different areas as detected by the semi-automated threshold algorithm. As shown in Fig. S1, the identified tumour areas delimited by the threshold t_{tumour} correspond well to the visual clinical tumour borders for the lesions. Also, the area corresponding to MAL-treated normal skin could be automatically delimited by the threshold t_{normal}, as illustrated for lesion I and II; however, as the application area of MAL for lesion III was larger than the imaging field of view, the border between MAL-treated and untreated skin could not be identified. In this case, an average value of the fluorescence outside the detected tumour area was applied as a value for the normal fluorescence in the further analysis. It can also be seen that the fluorescence pattern differs slightly between the first (row 2) and second (row 4) treatment. At the second treatment, the fluorescence of the MAL-treated perilesional skin has a more speckled structure (lesion I and II). This was observed in four of the 35 lesions.

In order to evaluate how well the semi-automated algorithm was able to demarcate the tumour, the visual clinical area (marked in the clinical photographs) was compared with the semi-automated detected tumour area from the fluorescence images. Fig. 2 shows a drop-line graph for the areas obtained for each lesion, i.e. the areas calculated based on the visual clinical margin and by the semi-automated threshold algorithm (three lesions excluded from analysis). As shown by the figure, the detected tumour area from the fluorescence images was in general substantially larger than the visually marked

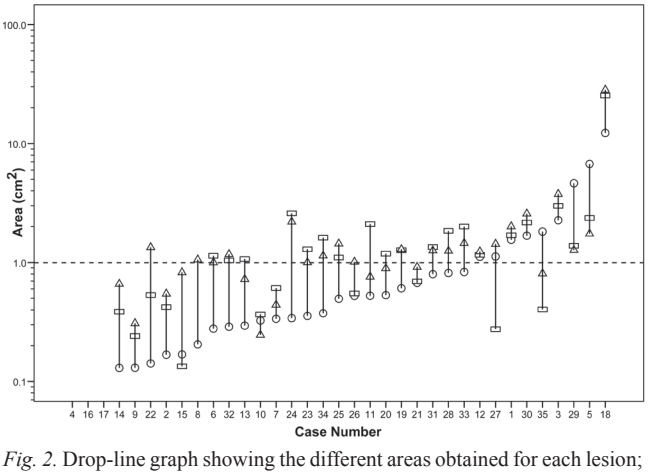

Fig. 2. Drop-line graph showing the different areas obtained for each lesion; circles "o" correspond to the area obtained by the clinical tumour margin, rectangles "□" correspond to the tumour areas obtained by the thresholding algorithm applied to the fluorescence images acquired at the first treatment and triangles "Δ" to the tumour areas obtained from the fluorescence images acquired at the second treatment. Three lesions (numbers 4, 16, and 17) were excluded from analysis as the images also contained areas with actinic keratoses.

tumour areas in the clinical photographs if the tumour was less than 1 cm^2 ($n = 18/23$). This can also be observed in Fig. S1, in which the fluorescence images (row 2) show a larger tumour area compared with the visual clinical tumour marking (row 1). The major deviation from this trend was found in lesions having a visual clinical tumour area larger than 1 cm^2 (Fig. 2), in which only three out of nine lesions showed a larger tumour area obtained in the fluorescence images. This implies that when investigating small BCCs with MAL-induced fluorescence, i.e. lesions less than 1 cm^2, the tumour area identified by the fluorescence will, in general, be larger than the area defined by the visual clinical marking. No significant difference in tumour area was observed comparing the fluorescence images obtained before the first and second PDT sessions.

The fluorescence contrast was calculated from the fluorescence images obtained after MAL application at both treatment visits (Fig. 3). As expected, the fluorescence contrast between tumour and MAL-treated normal skin was significantly higher than the contrast between MAL-treated normal skin and untreated skin. Interestingly, the mean tumour contrast was found to increase from 1.65 ± 0.06, obtained in connection with the first PDT session, to 1.84 ± 0.07 at the second treatment ($p < 0.01$), as shown by the figure. This implies that the accumulation of PpIX in the tumour is generally higher during the second PDT session.

Fluorescence images from BCCs treated with ALA were available from an earlier study by our group (14). Thus, it was possible to compare the fluorescence contrasts obtained using the two different pro-drugs, i.e. ALA and MAL, as presented in Fig. 4. As shown by the figure, the mean fluorescence contrast obtained during the first treatment with MAL (1.65 ± 0.06) was significantly higher than the mean fluorescence contrast obtained after a 3-hour application of ALA (1.20 ± 0.06). We also tried to implement the semi-automated thresholding algorithm on the ALA data; however, due to the low mean contrast value, the algorithm failed to find appropriate thresholds in the ALA images (data not shown). In our earlier study on ALA, we instead decided to calculate a peak contrast value including only 10% of the highest fluorescent pixels within the marked tumour area of all tumours. The value on the peak ALA contrast was found to be 1.61 ± 0.10. This value is similar to the mean contrast value obtained with MAL. Thus the mean contrast with MAL is as high as the peak contrast obtained with ALA.

At follow-up, 7–18 weeks after the last treatment, 32 lesions (91%) were completely cleared, two (6%) were partially cleared and one (3%) did not respond to PDT. No correlation between the fluorescence and lack of treatment response was observed; although, due to the small number of patients not responding to treatment in this study, no statistical analysis could be made. Furthermore, we investigated the correlation between the fluorescence and VAS, but no correlation was found (data not shown).

Adverse events

Adverse events were observed in three patients. Two patients had severe pain in the treated area, but this resolved without any action taken. One patient had a serious adverse event not related to the study presenting with hypotension, which resolved after half a day in hospital.

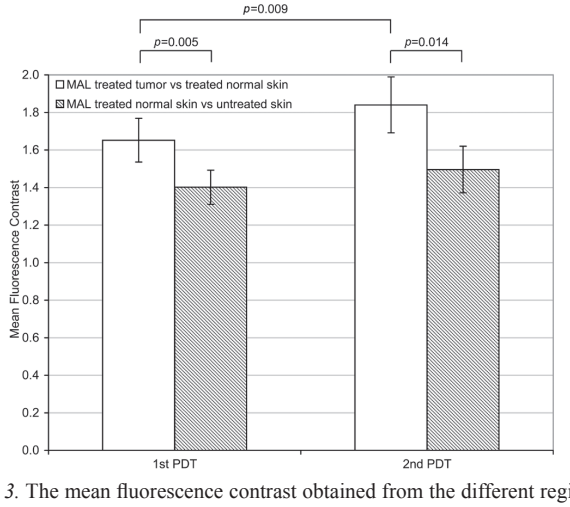

Fig. 3. The mean fluorescence contrast obtained from the different regions of the fluorescence images of basal cell carcinomas ($n = 32$) treated with methyl-aminolaevuninate (MAL). Open bars show the mean contrast values of MAL-treated tumour compared with MAL-treated perilesional normal skin. Filled bars show the mean contrast of MAL-treated perilesional normal skin compared with untreated skin. Error bars are 95% confidence intervals. Data obtained at the first and second treatment are presented.

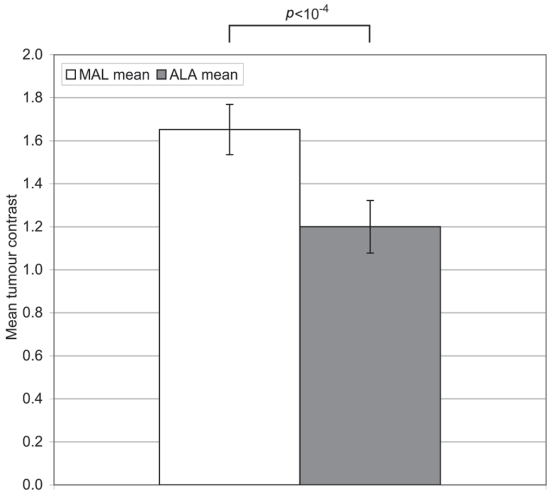

Fig. 4. Fluorescence data of basal cell carcinomas (BCCs) exposed to methyl-aminolaevuninate (MAL) (open bar) ($n = 32$) in the present study compared with those exposed to aminolaevulinic acid (ALA) (filled bar) ($n = 15$) in an earlier study (14). The values correspond to the mean fluorescence contrast in the tumour area. Error bars are 95% confidence intervals.

DISCUSSION

We have evaluated the fluorescence contrast between tumour and perilesional normal skin in BCCs undergoing two consecutive MAL-PDT sessions. It was found that the fluorescence contrast obtained at the second PDT session was, in general, significantly higher than at the first treatment, implying that the accumulation of PpIX in the tumour area is higher during the second PDT session. This is probably explained by increased penetration of the pro-drug, i.e. MAL, into the tumour due to disruption of the penetration barrier after the first treatment. The effect of PDT on the skin barrier function of non-melanoma skin cancer has been confirmed in rodents (18), but in humans the effect on PDT on skin barrier has been investigated only on patients with acne, where no effect on transepidermal water loss was found (19). The skin barrier differs between acne and skin tumours, since the latter already has an impaired skin barrier. In addition, the elevated PpIX levels at the second treatment could probably be explained by an effect on the skin barrier after the first treatment, as confirmed in rodents. Another possible explanation for the higher PpIX accumulation in the tumour area at the second PDT session might be the presence of inflammatory cells as a result of the first treatment. Inflammatory cells have been reported to show accumulation of PpIX after administration of ALA or MAL (18, 20). Thus, the presence of inflammatory cells at the second PDT session could also contribute to the higher accumulation of PpIX in the tumour region. Furthermore, the effect on the PpIX accumulation in the perilesional normal skin resulted in a more speckled fluorescence pattern at the second treatment for some lesions (4 out of 35). This effect could also be attributed to disruption of the penetration barrier or a gathering of inflammatory cells in the normal skin around the tumour.

A semi-automated image analysis algorithm was implemented to identify areas in the fluorescence images corresponding to the tumour and the surrounding normal skin. Our results show that the fluorescence-detected margins, in general, were larger than the visual clinical margins of the BCC detected on clinical photographs. Only the large tumours (>1 cm^2) deviated from this pattern. As no detailed histopathological mapping of the tumours was available, it is unclear whether the larger area actually corresponds to tumour. Higher accumulation of PpIX in close vicinity to the tumour mass has been reported previously (17, 21). Nevertheless, the result implies that, when investigating small BCCs (<1 cm^2) with MAL-induced fluorescence, the identified tumour area will be larger than the area defined by the visual border.

In this study, two lesions only partially cleared and one did not respond (6% and 3%, respectively). There is an ongoing quest to find the reasons to this resilience to treatment (7). One possible explanation could be the lack of accumulation of PpIX. In the present study, no deviation in fluorescence could be observed for the three lesions that did not clear completely. In our earlier study using a microdialysis technique, it was shown that therapeutic concentrations of ALA or MAL at depths between 1 and 2 mm were obtained in only 50% of the investigated lesions (22). It is possible that the lack of treatment effect might be related to lack of PpIX accumulation in deeper tissue layers. Thus, superficial fluorescence measurements might not always be useful to predict treatment outcome.

Although other authors have reported a correlation between the fluorescence and the pain experienced by patients during the irradiation phase of PDT (11), we could not observe any correlation between the fluorescence contrast and the recorded VAS levels among the patients in this study. However, the earlier report concerned actinic keratoses, so larger areas might have been treated. Since BCCs generally affect much smaller areas, the degree of photosensitization of the tumour is of much less importance for the pain sensation. This is in agreement with our earlier report, that pain is related to the size of the treatment area (23, 24).

The fluorescence contrast between the tumour and normal skin was found to be higher when using MAL compared with fluorescence data from our former study applying ALA as a pro-drug (14). The fluorescence contrast was measured in a similar manner in both studies. This is most likely explained by the fact that MAL has a low penetration into normal intact skin, while ALA generally has a higher penetration into intact skin (25, 26) leading to reduced tumour selectivity for ALA. No difference between penetration of MAL and ALA has been seen in BCCs (18, 22). This means that, when performing topical PDT using MAL, higher tumour specificity can be obtained. However, the penetration of the pro-drug is restricted to areas with decreased barrier function. This means that when performing PDT on tumours with an intact epithelium, ALA might be the pro-drug of choice. When it comes to FD, which is based on demarcating the tumour from the surrounding tissue, our results suggest that MAL is more suitable than ALA because of the higher tumour contrast. As most studies regarding FD for tumour demarcation have been performed using ALA, future studies investigating the histopathological correlation with MAL-FD are required.

ACKNOWLEDGEMENTS

We thank Sahlgrenska Academy at the University of Gothenburg and Sahlgrenska University Hospital for giving us the opportunity to perform this study. We also thank the Swedish Society of Medicine for financial support. The study was also financially supported by grants from the federal government under the ALF-agreement.

Conflict of interest: Carin Sandberg has received travel grants from Schering-Plough and Photocure and Christina Halldin has

received travel grants from Photocure. John Paoli has received fees for giving lectures from Meda, Leo Pharma, Schering-Plough, Astellas, he has also been in an advisory board for Meda and received travel grants from Photocure. Ann-Marie Wennberg has taken part in clinical trials with Galderma, PhotoCure, 3M and Fujisawa. She has received fees for giving lectures from Galderma, PhotoCure, 3M, Fujisawa and Schering-Plough, Olle Larkö has taken part in a clinical trial with Photocure.

REFERENCES

1. Leiter U, Garbe C. Epidemiology of melanoma and nonmelanoma skin cancer – the role of sunlight. Adv Exp Med Biol 2008; 624: 89–103.
2. Hoey SE, Devereux CE, Murray L, Catney D, Gavin A, Kumar S, et al. Skin cancer trends in Northern Ireland and consequences for provision of dermatology services. Br J Dermatol 2007; 156: 1301–1307.
3. Wassberg C, Thorn M, Johansson AM, Bergström R, Berne B, Ringborg U. Increasing incidence rates of squamous cell carcinoma of the skin in Sweden. Acta Derm Venereol 2001; 81: 268–272.
4. Katalinic A, Kunze U, Schafer T. Epidemiology of cutaneous melanoma and non-melanoma skin cancer in Schleswig-Holstein, Germany: incidence, clinical subtypes, tumour stages and localization (epidemiology of skin cancer). Br J Dermatol 2003; 149: 1200–1206.
5. Diepgen TL, Mahler V. The epidemiology of skin cancer. Br J Dermatol 2002; 146 Suppl 61: 1–6.
6. Tinghög G, Carlsson P, Synnerstad I, Rosdahl I. Societal cost of skin cancer in Sweden in 2005. Acta Derm Venereol 2008; 88: 467–473.
7. Braathen LR, Szeimies RM, Basset-Seguin N, Bissonnette R, Foley P, Pariser D, et al. Guidelines on the use of photodynamic therapy for nonmelanoma skin cancer: an international consensus. J Am Acad Dermatol 2007; 56: 125–143.
8. Morton CA, Brown SB, Collins S, Ibbotson S, Jenkinson H, Kurwa H, et al. Guidelines for topical photodynamic therapy: report of a workshop of the British Photodermatology Group. Br J Dermatol 2002; 146: 552–567.
9. Kennedy JC, Pottier RH. Endogenous protoporphyrin IX, a clinically useful photosensitizer for photodynamic therapy. J Photochem Photobiol B 1992; 14: 275–292.
10. Wang I, Bendsoe N, Klinteberg CA, Enejder AM, Andersson-Engels S, Svanberg S, et al. Photodynamic therapy vs. cryosurgery of basal cell carcinomas: results of a phase III clinical trial. Br J Dermatol 2001; 144: 832–840.
11. Wiegell SR, Skiveren J, Philipsen PA, Wulf HC. Pain during photodynamic therapy is associated with protoporphyrin IX fluorescence and fluence rate. Br J Dermatol 2008; 158: 727–733.
12. Kennedy JC, Marcus SL, Pottier RH. Photodynamic therapy (PDT) and photodiagnosis (PD) using endogenous photosensitization induced by 5-aminolevulinic acid (ALA): mechanisms and clinical results. J Clin Laser Med Surg 1996; 14: 289–304.
13. Stenquist B, Ericson MB, Strandeberg C, Mölne L, Rosén A, Larkö O, et al. Bispectral fluorescence imaging of aggressive basal cell carcinoma combined with histopathological mapping: a preliminary study indicating a possible adjunct to Mohs micrographic surgery. Br J Dermatol 2006; 154: 305–309.
14. Ericson MB, Sandberg C, Gudmundson F, Rosén A, Larkö O, Wennberg AM. Fluorescence contrast and threshold limit: implications for photodynamic diagnosis of basal cell carcinoma. J Photochem Photobiol B 2003; 69: 121–127.
15. Andersson-Engels S, Canti G, Cubeddu R, Eker C, af Klinteberg C, Pifferi A, et al. Preliminary evaluation of two fluorescence imaging methods for the detection and the delineation of basal cell carcinomas of the skin. Lasers Surg Med 2000; 26: 76–82.
16. Juzeniene A, Juzenas P, Iani V, Moan J. Topical application of 5-aminolevulinic acid and its methylester, hexylester and octylester derivatives: considerations for dosimetry in mouse skin model. Photochem Photobiol 2002; 76: 329–334.
17. Fritsch C, Homey B, Stahl W, Lehmann P, Ruzicka T, Sies H. Preferential relative porphyrin enrichment in solar keratoses upon topical application of delta-aminolevulinic acid methylester. Photochem Photobiol 1998; 68: 218–221.
18. de Bruijn HS, Meijers C, van der Ploeg-van den Heuvel A, Sterenborg HJ, Robinson DJ. Microscopic localisation of protoporphyrin IX in normal mouse skin after topical application of 5-aminolevulinic acid or methyl 5-aminolevulinate. J Photochem Photobiol B 2008; 92: 91–97.
19. Faurschou A, Wiegell SR, Wulf HC. Transepidermal water loss after photodynamic therapy, UVB radiation and topical corticosteroid is independent of inflammation. Skin Res Technol 2007; 13: 202–206.
20. Castano AP, Mroz P, Hamblin MR. Photodynamic therapy and anti-tumour immunity. Nature Reviews 2006; 6: 535–545.
21. Collaud S, Juzeniene A, Moan J, Lange N. On the selectivity of 5-aminolevulinic acid-induced protoporphyrin IX formation. Curr Med Chem Anticancer Agents 2004; 4: 301–316.
22. Sandberg C, Halldin CB, Ericson MB, Larkö O, Krogstad AL, Wennberg AM. Bioavailability of aminolaevulinic acid and methylaminolaevulinate in basal cell carcinomas: a perfusion study using microdialysis in vivo. Br J Dermatol 2008; 159: 1170–1176.
23. Grapengiesser S, Ericson M, Gudmundsson F, Larkö O, Rosén A, Wennberg AM. Pain caused by photodynamic therapy of skin cancer. Clin Exp Dermatol 2002; 27: 493–497.
24. Sandberg C, Stenquist B, Rosdahl I, Ros AM, Synnerstad I, Karlsson M, et al. Important factors for pain during photodynamic therapy for actinic keratosis. Acta Derm Venereol 2006; 86: 404–408.
25. Bender J, Ericson MB, Merclin N, Iani V, Rosén A, Engström S, et al. Lipid cubic phases for improved topical drug delivery in photodynamic therapy. J Control Release 2005; 106: 350–360.
26. Wiegell SR, Stender IM, Na R, Wulf HC. Pain associated with photodynamic therapy using 5-aminolevulinic acid or 5-aminolevulinic acid methylester on tape-stripped normal skin. Arch Dermatol 2003; 139: 1173–1177.